

# Optical Fiber Sensors Based on Lossy Mode Resonances

Miguel Hernández, Carlos R. Zamarreño, Ignacio Del Villar, Francisco J. Arregui, and Ignacio R. Matias

Public University of Navarre, 31006 Pamplona, Spain

## 1 Introduction

In the last decades, optical fiber sensors have played an important role in niche applications because of their advantages over electronic sensors. First of all, optical fiber makes possible the multiplexing of a large amount of sensor data over long distances. This feature allows placing the sensing devices at kilometers from the electronic systems used to process the information. In addition, optical fiber is made of dielectric materials. Consequently, optical fiber sensors are not affected by electromagnetic fields, what makes them suitable to be used in situations under high electromagnetic fields or radiation doses [1]. Furthermore, this technology can be also used in medical applications due to its biocompatibility and has acquired a great importance in the development of biomedical instrumentation. Other interesting advantages of optical fiber sensors are their small size or their wide temperature working range [2-5].

Due to these interesting features, several optical fiber sensing architectures have been developed in the last decades. Just to mention some examples, there are optical fiber sensors based on fiber Bragg gratings (FBGs) [6], long period gratings (LPGs) [7], photonic crystal fibers (PCF) [8], tapered fibers [9], interferometers [10], electromagnetic resonances [11-15], etc...

In addition, the development of novel materials and deposition methods on the nanometric scale has meant an important breakthrough in different fields [16, 17]. More specifically, in the field of optical fiber sensors, nanostructured coatings allow the generation of optical effects that are not appreciable with the utilization of thick films. Electromagnetic resonances, such as surface plasmon resonances (SPR) or lossy mode resonances (LMR), that make possible the development of optical fiber sensors with tunable spectral response, are a good example of these new phenomena [18].

Among this variety of optical fiber techniques, SPR is one of the most widely studied. Since the first sensing application of SPR was reported in 1983 [19], a lot of structures based on this phenomenon have been developed, becoming a standard in the design and fabrication of sensors and biosensors.

This phenomenon consists of the excitation of a surface plasmon wave at the metal-dielectric interface. When some particular conditions of the incident and the surface plasmon wave match, a resonance is generated and a sharp absorption peak can be observed in the transmitted light. The resonance wavelength depends

on the refractive index of the material in contact with the metal. In other words, a change in this refractive index will produce a wavelength shift of the resonance peak [14]. This fact has been applied in the design and fabrication of sensors for different applications [20-27].

First studies about SPR used a complex optical setup (known as the Kretschmann configuration), including a prism, to excite the surface plasmon wave. This setup presents some important drawbacks, such as its big size and the presence of fragile mechanical parts. The optical fiber configuration, developed by Jorgenson and Yee [28], overcomes these disadvantages and allows the miniaturization of these devices, adding these features to the typical advantages of optical fiber sensors [29-32]. As a result, numerous optical fiber sensors based on SPR have been developed in the last years [11-13,33-39].

However, SPR-based devices have some limitations. Firstly, there are just a few stable metals that allow the generation of SPR in the visible and near-infrared spectral regions, such as gold or silver, and they are expensive. In addition, SPR is only visible with TM polarization of light, what makes necessary the use of a polarizer and an optical fiber that maintains the polarization to obtain a sharp absorption peak. Moreover, the conditions for SPR generation are very specific and for this reason, SPR is produced in a limited spectral region that depends on the deposited metal.

Recently, the use of metallic oxides to generate optical devices based on the Kretschmann configuration, have allowed the opening of this technology to new materials, such as Indium Tin Oxide (ITO) [40-43]. This fact allows overcoming the drawback of using only metals to obtain SPRs. The initial objective of this study was to generate electromagnetic resonances by depositing ITO coatings onto optical fiber. When this aim was achieved, a deeper study of the bibliography revealed that the obtained resonances were not SPRs, but Lossy Mode Resonances (LMR). These LMRs are a type of resonances that overcomes some of the limitations of SPRs and never had been observed before in an optical fiber configuration. In fact, more than twenty-two publications have been devoted to this topic in the last two years.

The phenomenon of LMR will be presented and analyzed in this chapter. Theoretical basis of LMR will be explained and the differences between this novel resonances and SPR will be demonstrated, emphasizing the advantages of LMR over SPR.

## **2 Lossy Mode Resonances (LMR)**

When an optical waveguide is coated by a thin-film (see Fig. 1), the propagation of light is affected. If the refractive index of the coating has an imaginary part different to zero, it introduces losses that can produce electromagnetic resonances. Depending on the properties of the different materials involved in the system (the waveguide, the coating and the external medium), three different cases of electromagnetic resonances can be distinguished [44].

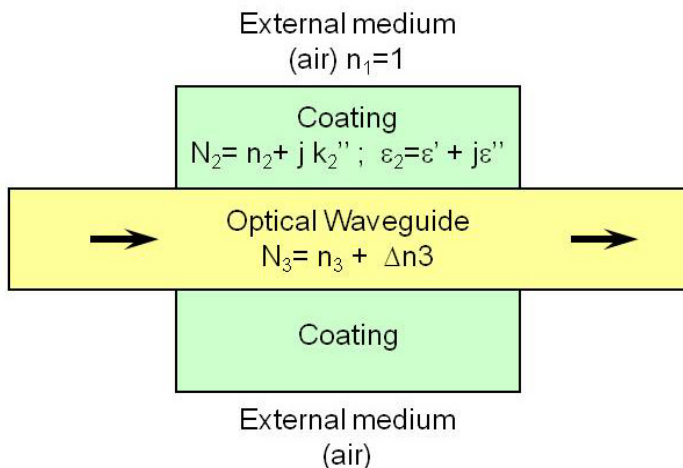


**Fig. 1.** Schematic representation of the optical system used to obtain electromagnetic resonances

The first case occurs when the real part of the thin-film permittivity is negative and higher in magnitude than both its own imaginary part and the permittivity of the material surrounding the thin film (i.e. the optical waveguide and the surrounding medium in contact with the thin film). In this case, coupling occurs between light propagating through the waveguide and a surface plasmon, which is called Surface Plasmon Polariton (SPP). This phenomenon produces a resonance called Surface Plasmon Resonance (SPR).

The second case occurs when the real part of the thin-film permittivity is positive and higher in magnitude than both its own imaginary part and the permittivity of the material surrounding the thin film. Some authors consider these modes as long-range guided modes [44], whereas others call them lossy modes [45, 46]. In this work, they will be called lossy modes to make a difference between them and the rest of guided modes. These lossy modes will produce the second type of resonances: the Lossy Mode Resonance (LMR).

Finally, the third case occurs when the real part of the thin-film permittivity is close to zero, while the magnitude of its imaginary part is large [44]. This case, known as long-range surface exciton polariton (LRSEP), falls beyond the scope of this study and will no longer be studied.

The permittivity of a material can be expressed in terms of its complex refractive index ( $N=n+jk$ ) according to Eq. 1.

$$\varepsilon = \varepsilon' + j\varepsilon'' = N^2 = (n + jk)^2 = n^2 - k^2 + j2nk \quad (1)$$

And, finally,

$$\begin{aligned} \varepsilon' &= n^2 - k^2 \\ \varepsilon'' &= 2nk \end{aligned} \quad (2)$$

Thus, having the device schematically represented in Fig. 1 and the relations from Eq. 2, the conditions needed to obtain the different types of electromagnetic resonance (SPR, LMR and LRSEP) can be expressed in terms of the refractive index of the different materials involved in the system.

In Table 1 a summary of these conditions is presented, considering the case in which  $n_2 > 0$  and  $k_2 < 0$ .

**Table 1.** Summary of the conditions needed to obtain the different types of electromagnetic resonances with the system represented in Fig.1.

Resonance	Permittivity	Refractive Index
Surface Plasmon Resonance <b>SPR</b>	$\epsilon_2' < 0$ $\epsilon_2' > \epsilon_2''$ $\epsilon_2' > \epsilon_3'$	$ n_2  <  k_2 $ $n_2 > (1-\sqrt{2})k_2$
Lossy Mode Resonance <b>LMR</b>	$\epsilon_2' > 0$ $\epsilon_2' > \epsilon_2''$ $\epsilon_2' > \epsilon_3'$	$ n_2  >  k_2 $
Long-Range Surface Exciton Polariton <b>LRSEP</b>	$\epsilon_2' \approx 0$ $\epsilon_2'' \uparrow \uparrow$	$ n_2  \approx  k_2 $ $2nk \uparrow \uparrow$

Although not too many studies have been published about LMR, there are some theoretical studies devoted to light propagation through semiconductor-cladded waveguides [47, 48]. The characteristics of these materials are adequate for generation of lossy modes. Moreover, attenuation maxima of the light propagating through the waveguide are obtained for specific thickness values [47]. This effect is produced as a consequence of a coupling between a waveguide mode and a particular lossy mode of the semiconductor thin film.

This coupling depends on two conditions: a considerable overlap between the mode fields and the phase-matching condition is sufficiently satisfied (i.e., the real parts of propagation constants are equal) [45]. Both conditions occur when modes propagating through the waveguide are near the cutoff condition. This cutoff condition sets the point in which a mode starts to be guided through the coating, and it is conditioned by two parameters: the wavelength and the coating thickness. Since the phenomenon occurs when the lossy mode is near cutoff, there are cutoff thickness values that lead to attenuation maxima [47]. For a fixed wavelength, as the thickness of the thin film on the waveguide is increased, some modes guided in the optical waveguide become guided in the film, which causes a modal redistribution or modal conversion [48, 49].

Previous studies have been focused on the variation of thickness. However, if the thin-film thickness is fixed, a resonance will be visible in the electromagnetic spectrum for those incident wavelength values where there is a mode near cut-off in the overlay. This is of great interest because one of the basic ways of using waveguides as sensors is by analysis of resonance wavelength shift. Hence, the

phenomenon studied here is the generation of resonances in the electromagnetic spectrum based on near cut-off lossy modes. The right term should be Near Cutoff Lossy Mode Resonance (NCLMR). However, for the sake of simplicity the term Lossy Mode Resonance (LMR) will be used, which indeed is similar to that mentioned in [46].

Finally, it is worthy to note the differences between these two types of resonances, LMR and SPR. The first difference is that they are generated under different optical conditions (see Table 1). Some materials present a complex refractive index which divides the spectrum in two regions, as it is the case of ITO which will be explained later. Hence, these materials are able to generate both LMR and SPR depending on the spectral region. However, other materials just present one of the spectral regions, and for this reason, they generate either SPR or LMR. Other remarkable question is that LMR allows the generation of multiple resonances as the thickness of the coating is increased. However, SPR presents only one resonance, and it disappears when the coating thickness reaches a certain value. This property makes LMR appropriate for fabricating multi-peak sensors with a better sensitivity and multiple- wavelength optical filters. In Table 2, a summary of the differences between LMR and SPR is shown.

**Table 2.** Main differences between lossy mode resonances and surface plasmon resonances

	SPR	LMR
Region of the spectrum	High-reflectance region	Low-reflectance region
Supporting coating	Metallic	Metallic or dielectric
Resonance Peaks	Single	Multiple

## 2.1 Optical Fiber Configuration

To perform this study, a new optical fiber transmission configuration was developed in order to characterize the novel LMR-based devices. This setup is based in an idea previously reported by Jorgenson and Yee [28] used to work with SPR-based optical fiber sensors. This Jorgenson's configuration is an adaptation to optical fiber of the well known Kretschmann configuration [13, 41, 43, 50]. This adaptation overcomes some of the inconveniences of Kretschmann model, such as the complexity of the setup and the need of an optical prism. Moreover,

the new setup presents the general advantages related to optical fiber sensors (immunity to electromagnetic interferences, biocompatibility, low weight, small size, high sensitivity...).

As it can be seen in Fig. 2, light is launched into the optical fiber and it is collected at the other end of the fiber by a spectrometer.

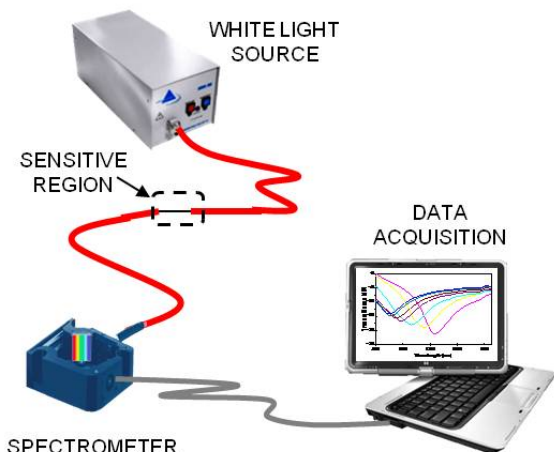


**Fig. 2.** Optical fiber configuration used to obtain and characterize the different resonances

In the middle of the optical path, there is a region where the optical fiber core is coated with the LMR supporting material. Cross section and longitudinal section of this region are shown in Fig. 3.

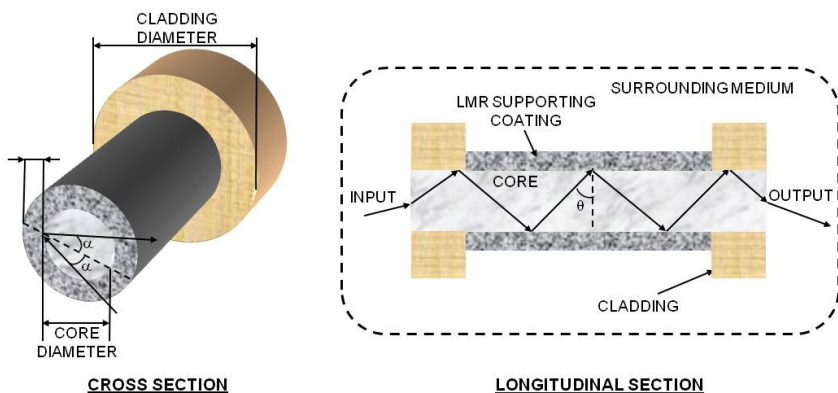


**Fig. 3.** Detail of the LMR supporting region. The cladding is chemically removed and the LMR supporting material is directly deposited onto the optical fiber core.

### 3 Optical Fiber Sensors Based on LMR

#### 3.1 Devices Based on a Single Coating

Different devices can be designed and fabricated by following the scheme shown in Fig. 3, where a single coating of a LMR supporting material has been deposited directly onto the optical fiber core.

##### 3.1.1 Optical Fiber Refractometers Based on ITO Coatings

ITO (Indium Tin Oxide) belongs to transparent conductive oxides (TCOs), which have been widely used in many scientific areas during the last decades: fabrication of heat shields, liquid crystal displays, flat panel displays, plasma displays, touch panels, electronic ink, organic light-emitting diodes, solar cells, antistatic coatings or even electromagnetic interference shields [51, 52]. This success is due to the good qualities that these materials present (electrochemical stability and high transmittance in the visible spectral range), if compared with other well-known conductive materials such as gold or silver. More specifically, ITO has been also used in many different sensing applications such as the fabrication of conductimetric or optical sensors [53-57], by exploiting the combination of conductive and transparency/reflectivity properties in the visible/infrared region respectively.

In fact, it is this dual behavior what makes ITO an adequate candidate for the simultaneous generation of SPR and LMR as well [18]. In Fig. 4, the optical properties of the ITO used in this work are shown. In the spectral region between 3-4.5  $\mu\text{m}$ , the imaginary part of the ITO refractive index is of the order of metals. Consequently, this region is adequate for SPR generation. However, for the spectral region from 0.5-2  $\mu\text{m}$ , the imaginary part is lower and permits the LMR generation, according to the conditions cited in Table 1.

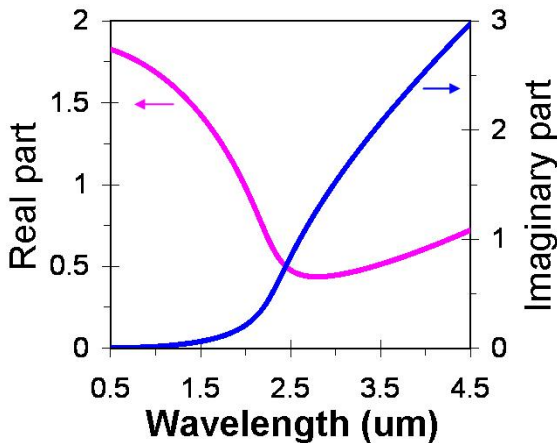


**Fig. 4.** Complex refractive index of ITO. Real part  $n$  (pink) and imaginary part  $k$  (blue) [18].

Moreover, the ITO coating features can be modified by introducing simple variations in the fabrication process. This fact allows tuning the resonance region. In other words, the resonance can be placed in the visible or in the infrared region, depending on the ITO characteristics.

The performance of the device as a refractometer was tested by obtaining the transmission response of the system for several surrounding media refractive indices: 1.321, 1.339, 1.358, 1.378, 1.400, 1.422 and 1.436, which were obtained from different water/glycerin concentration solutions from 0% to 85% respectively [58, 59].

### Single LMR Generation

The transmission spectra obtained are represented in Fig. 5a and 5b for ITO thickness values of 115 nm and 220 nm, respectively [18]. The plots presented in each figure correspond to different refractive index values of the outer medium, as indicated previously. A resonance is observed in all spectra.

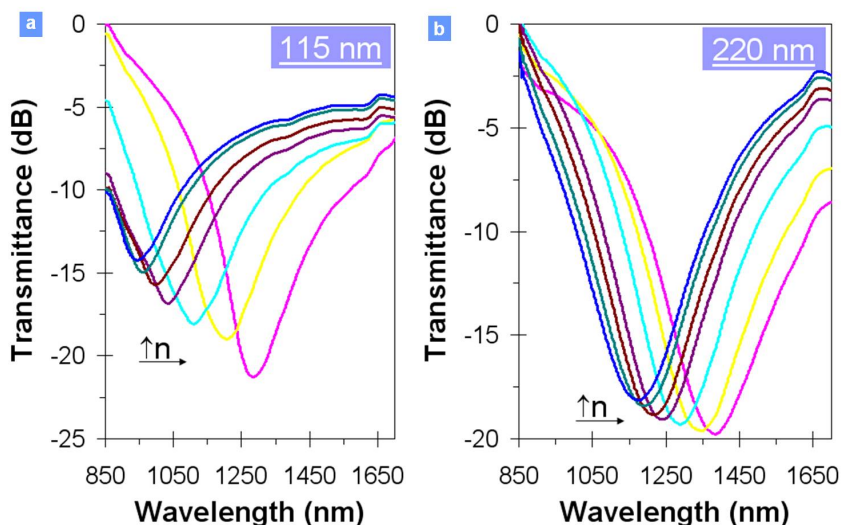


**Fig. 5.** Experimental results of LMR sensitivity versus surrounding medium refractive index: transmission spectra obtained when the ITO-coated region is immersed in different refractive index solutions for different ITO layer thickness values: a) 115 nm b) 220 nm [18]

Here, it is important to note that as the refractive index increases there is an optical redshift of the resonance. In addition to this, as the coating thickness increases, the sensitivity (i.e. the resonance shift depending on the surrounding refractive index) is reduced. In other words, the thickness can be used for controlling the sensitivity of the device, which is 2956 nm per refractive index unit (RIU) for the sensor coated with a 115 nm film and 1826 nm per RIU for the sensor coated with a 220 nm coatings. These values are in the range of the state of

art SPR sensors [60]. This effect can be clearly observed in Fig. 6, where the resonance wavelengths are shown as a function of the refractive index of the surrounding medium.

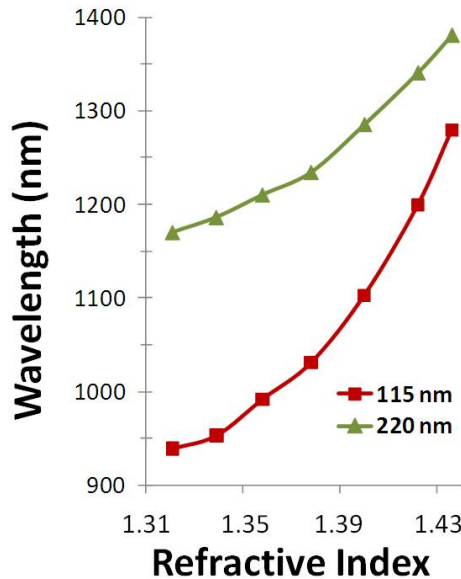


**Fig. 6.** Evolution of the theoretical (a) and experimental (b) LMR absorption peaks observed in Fig. 9 and 10 when the refractive index of the external medium changes

### *Multiple LMR Generation*

It was observed in Fig. 5 and 6 that when the ITO thickness is increased, the sensitivity of an LMR to the surrounding refractive index decreases. In this section, a second effect of the variation of the ITO thickness will be presented. According to [47] and [49], there are attenuation maxima in the light transmitted through a coated optical fiber as a function of the coating thickness. These maxima coincide with a near cut-off mode in the coating. The same conclusion should be valid for the generation of LMR in the transmission spectrum. For specific wavelength values there are near cutoff modes in the coating. So far a single LMR has been visualized. However, if the ITO thickness is increased there should be more modes guided in this region. The consequence would be the generation of multiple LMR resonances. To prove this hypothesis, in Fig. 7 the response when the ITO thickness is 440 nm are presented.

Three different LMR can be distinguished in the transmission spectra when the surrounding refractive index is 1.321. These results prove the multiple LMR generation. The phenomenon can be exploited for the generation of multiple wavelength filters and sensors with multiple points of reference.

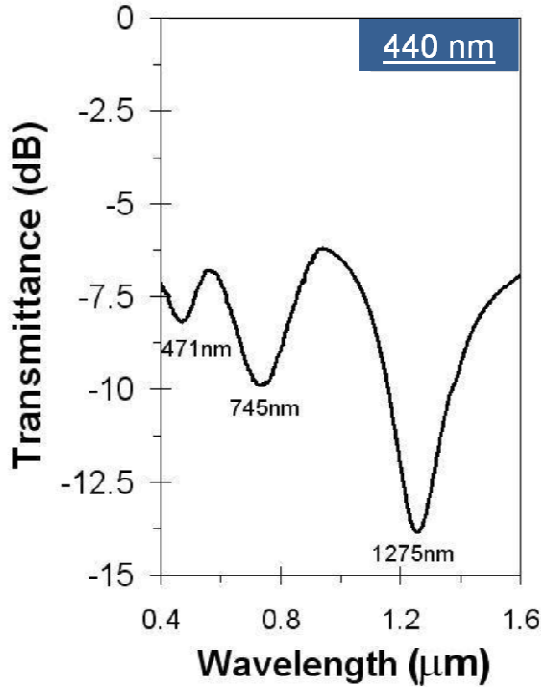


**Fig. 7.** Multiple LMR: Transmission spectrum obtained for an ITO layer thickness of 440 nm [18]

### 3.1.2 Optical Fiber pH Sensor Based on a PAH/PAA Thin-Film Deposited onto the Optical Fiber Core

As it was advanced before, LMR can be generated by very different materials. In this section, the capability of PAH/PAA (poly(allylamine hydrochloride) / poly(acrylic acid)) polymeric films to support LMR is presented. With this aim, 100 bilayers of these materials were deposited directly onto the optical fiber core. The LbL method was used to complete this process [61]. The evolution of the transmission spectra obtained during the deposition is shown in Fig. 8, where the generation of 3 different absorption peaks can be observed.

This way, the generation of LMR with polymeric coatings had been demonstrated. But the PAH/PAA structure is not only able to generate LMRs. In addition, if the coating is dipped into liquid solutions, its thickness can be modified as a function of the external medium pH. This effect has been named in previous works as *swelling/deswelling* phenomenon [62, 63]. Taking into account this feature, the behavior of these devices as pH sensors was tested. With this purpose, a device consisting of 25 bilayers of PAH/PAA was fabricated. The first LMR of this device was centered in the 400-1000 nm region.

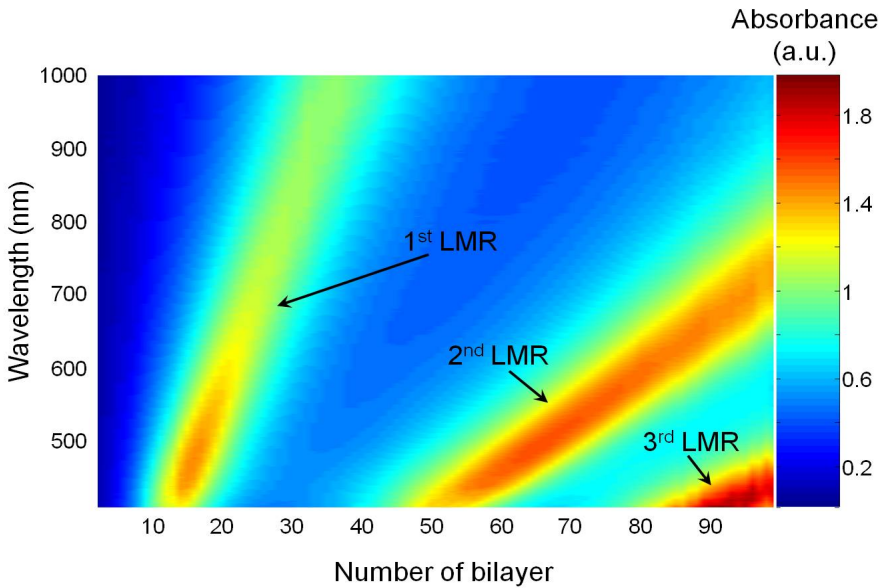


**Fig. 8.** Evolution of the transmitted spectra during the deposition of the PAH/PAA coating [61]

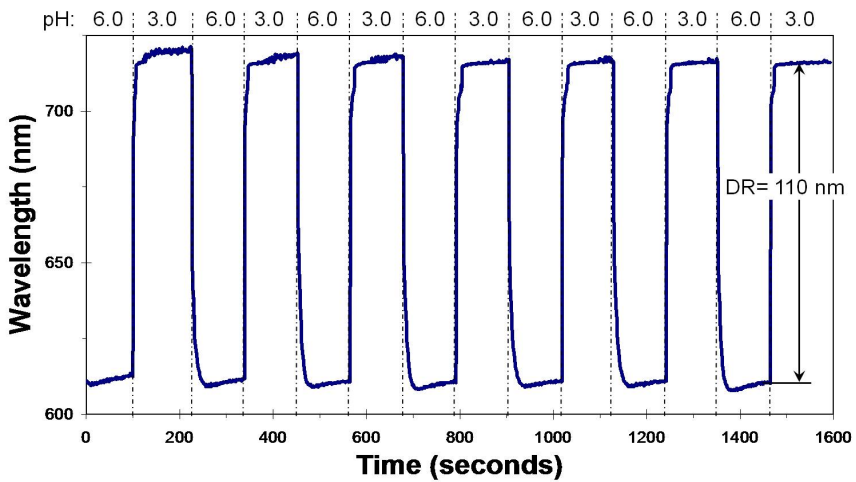


**Fig. 9.** Dynamical response of the sensing device when it is alternately immersed into solutions at pH 3 and 6 [61]

In Fig. 9 the shift of the LMR absorption peak is shown when the sensitive coating is alternately immersed into solutions at pH 3 and 6. The response is highly stable and repetitive. The absorption peak shows a shift of 110 nm in the tested pH range, what is equivalent to a sensitivity of 36.6 nm/pH unit. In addition, this device presents rise and fall times of 24 and 33 seconds, respectively [61].

Additionally, in order to observe the resonance wavelength shift for intermediate pH values, the device was exposed to repeated cycles of pH 6, 5, 4 and 3. In Fig. 10 it is represented the resonance wavelength shift as a function of time showing a durable and repetitive response for several pH change cycles between pH 6 and pH 3 [61].

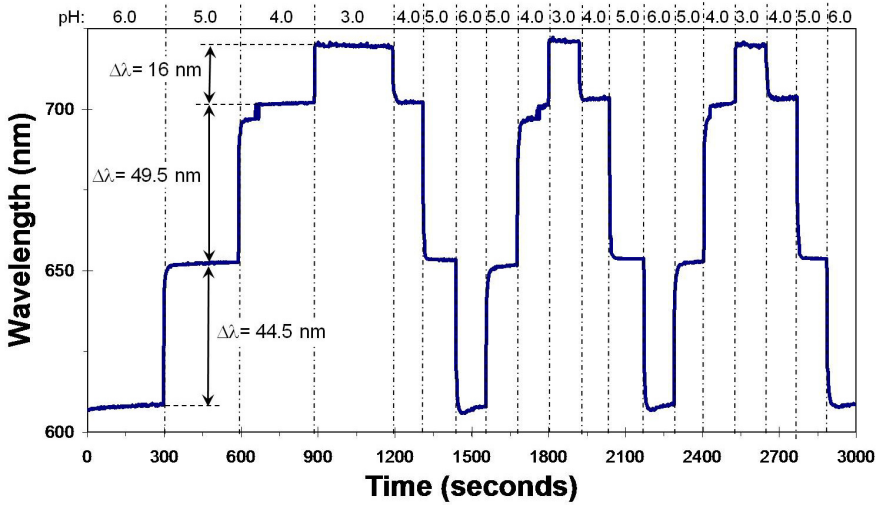


**Fig. 10.** Dynamical response of the sensor to cycles of pH 6, 5, 4 and 3 of different duration [61]

Here, it is observed that the sensitivity between pH 6 and pH 5 (45.45 nm/pH unit) is of the same order than that between pH 5 and pH 4 (50 nm/pH unit). However, the sensitivity between pH 4 and pH 3 (16.12 nm/pH unit) is about three times lower than that of the rest, which indicated smaller coating thickness variations.

### 3.2 *Devices Based on Two Coatings: A LMR Supporting Coating and a Sensitive Coating*

It has been observed in section 3.1.1 that the LMR peaks shift to the red when the refractive index of the external medium varies. If the LMR supporting layer (the ITO layer in our case) is coated with any material whose effective refractive index is sensitive to a certain magnitude, the LMR absorption peaks generated by the ITO coating will shift when this external magnitude varies. This way, different optical fiber sensors can be fabricated by just adding a coating of a sensitive material onto the LMR supporting layer. Some examples of this procedure are shown in the following sections.

### 3.2.1 Optical Fiber Humidity Sensor Based on an Agarose Sensitive Layer Deposited onto an ITO LMR-Supporting Layer

Agarose is the substance used to fabricate the sensitive layer of this first sensor based on LMR. The thickness of this gel varies with the external relative humidity (RH) [64]. In fact, the agarose layer becomes thicker when the RH rises because the structure receives water molecules that take up the place where there was air before. As the water refractive index ( $n = 1.33$ ) is higher than the air ( $n = 1$ ), the effective refractive index of the agarose will be higher when the RH rises. [65]. A schematic detail of the device is shown in Fig. 11.

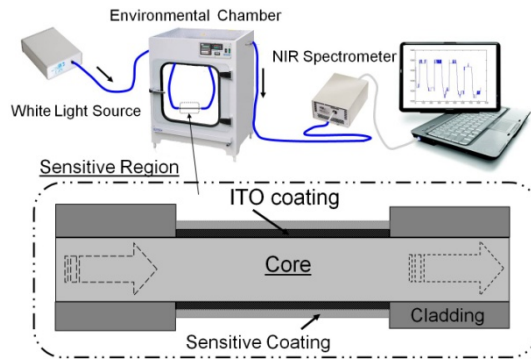


**Fig. 11.** Experimental setup utilized to characterize the sensor response and schematic detail of the sensitive region [66]

The experimental transmission setup used to characterize the sensor is also shown in Fig. 11. In order to subject the sensor to RH changes, the sensitive section was introduced into a climatic chamber.

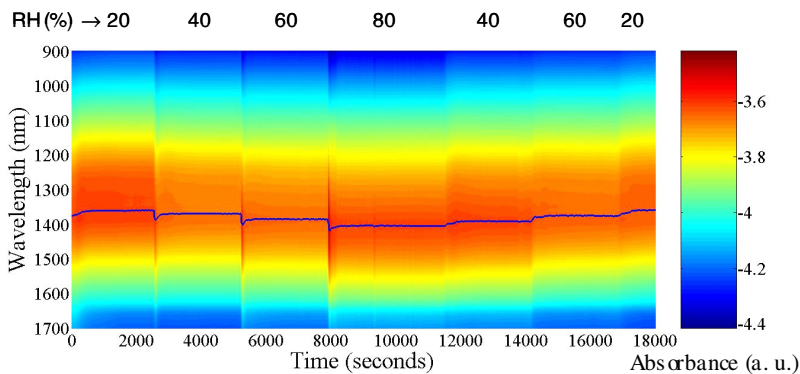


**Fig. 12.** Spectral response and maxima absorption wavelength variations (line) at different RH values [67]

The final device, that includes the agarose layer onto the ITO coating, shows a good sensitivity to changes in the external RH. This fact was tested by subjecting the sensor to a complete cycle of RH variation between 20 and 80%, with steps of 20% each 30 minutes [67].

In Fig. 12 the shift of the LMR absorption peak to higher wavelengths when the RH increases is shown. This figure represents the spectra collected during the experiment. The relative humidity is shown at the top of the graph and the time in seconds at the bottom, in the horizontal axis. The vertical axis represents the wavelength of the spectra. The colours chosen to represent the spectra are shown in the plot on the right. According to this palette, the red zones of the graph correspond to the LMR absorption peak. In order to show with higher clarity the evolution of the LMR, the maxima of these spectra have been remarked by a blue line. These experimental results corroborate the previous hypothesis about the variation of the agarose refractive index.

The dynamical response of the LMR maxima is shown with higher detail in figure 13. It can be observed here the shift of the LMR (blue line) with the changes in the RH (pink line). The sensor shows a dynamical range of 45 nm when the RH varies between 20 and 80%, what corresponds to a sensitivity of 0.75 nm/RH%.

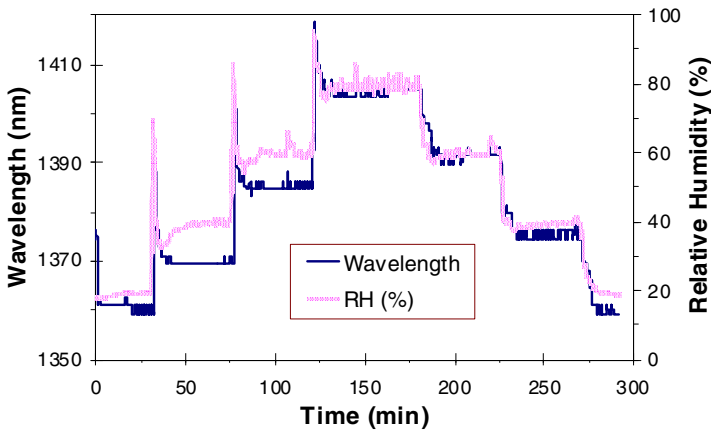


Fig. 13. Wavelength resonance when the sensor is subjected to RH changes [67]

### 3.2.2 Optical Fiber Humidity Sensor Based on a PAH/PAA Thin Film Deposited onto an ITO LMR-Supporting Coating

The agarose sensor presented in the previous paragraph shows a good response to humidity changes. However, the method applied to deposit the agarose onto the ITO layer makes difficult to control the thickness of the film. For this reason, it is only possible to select the sensor sensitivity and operation wavelength by changing the parameters of the ITO coating.

Another possibility is to find a different material to create the sensitive layer onto the ITO coating. The structure PAH/PAA presented in section 3.1.2 shows hydrophilic features and is sensitive to changes in the relative humidity. [6, 10, 68]. As the agarose gel, the PAH/PAA structure changes air by water when the RI rises, making higher its effective refractive index. But maybe the most important advantage of this structure is that the thickness of the deposited coating can be controlled with high accuracy.

To fabricate this humidity sensor, the refractometer based on an ITO coating with a thickness of 115 nm was used again. Two different sensors were fabricated by depositing onto the ITO coating two PAH/PAA coatings with different thickness values (sensor A with 20 bilayers of PAH/PAA and sensor B with 100 bilayers) [66].

Both sensors were tested for RH changes between 20% and 90% for several cycles using the experimental setup of Fig. 11. In both cases the resonance wavelength shift as a function of the RH follows perfectly the RH measurements obtained from the electronic sensor located in the climatic chamber. In addition to this, the sensor exhibits a fast response to changes in RH as it is shown in Fig. 14. Sensor A shows a variation of the resonance wavelength in the range studied of 13 nm, which corresponds to a sensitivity of 0.185 nm/RH%.

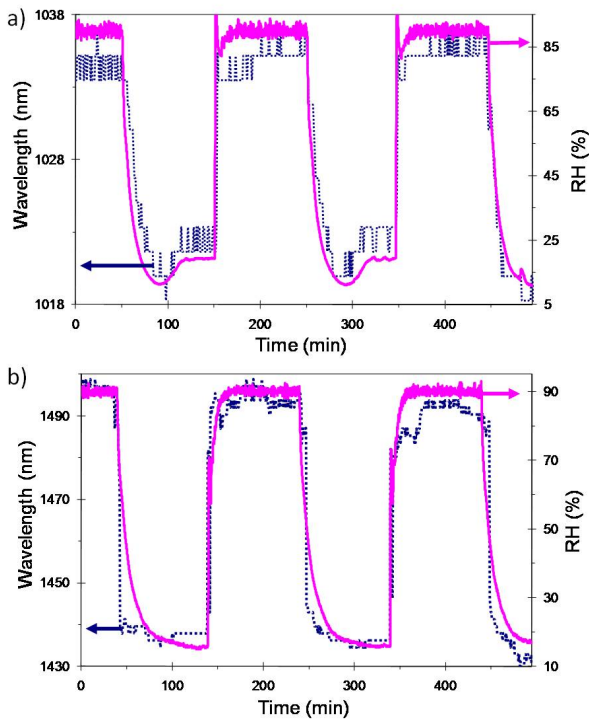


**Fig. 14.** Dynamical response of the sensors to changes in the RH of the external medium: a) sensor A (20 PAH/PAA bilayers) and b) sensor B (100 PAH/PAA bilayers) [66]

Similarly, in Fig. 14b, the dynamic response of sensor B to changes in RH from 20% to 90% is shown. As it can be seen, the dynamic range of this sensor in the studied range is 58 nm, which corresponds to a sensitivity of 0.83 nm/RH%.

This way, sensor B improves the characteristics of sensor A more than four times enabling the fabrication of OFHS suitable to be used in practical RH monitoring applications.

## 4 Conclusions

In this chapter, the theoretical basis of electromagnetic resonances produced when an optical waveguide is coated by a thin-film has been explained and the conditions needed to obtain the different types of resonance have been described. In particular, the phenomenon of Lossy Mode Resonance using an optical fiber configuration has been presented for the first time in the literature.

In order to distinguish this effect from the Surface Plasmon Resonance, their properties have been demonstrated.

In addition, the behavior of the different devices based on LMR as refractometers has been experimentally tested. It was observed that the wavelength of the LMR is sensitive to the refractive index of the external medium. In other words, the LMR peaks shift to higher wavelengths when the refractive index is increased. In addition, the sensitivity of this shift is higher when the thickness of the coating is lower.

This sensitivity to the refractive index of the external medium opens the door to a wide range of applications in the optical fiber sensors field. Any of these refractometers can be coated with a material whose refractive index is sensitive to a certain magnitude or substance. This way, a variation of this magnitude will produce a change in the refractive index of the sensitive material and, as a consequence, a shift in the LMR obtained. Some examples of sensors based on this technique have been presented and analyzed here in order to demonstrate this fact. In particular, different optical fiber humidity and pH sensors based on LMR have been characterized.

To summarize, a new kind of optical fiber sensors have been presented in this work. Taking into account the success of optical fiber sensors based on SPR, and due to the fact that some of their limitations are overcome by LMR sensors, this new phenomenon could be applied in a wide range of applications in the next years.

**Acknowledgements.** This work was supported by the Spanish Economy and Competitiveness Ministry TEC2010-17805 and AIB2010NZ-00328 Research Grants.

## References

- [1] Gusarov, A., Fernandez Fernandez, A., Vasiliev, S., Medvedkov, O., Blondel, M., Berghmans, F.: Effect of gamma-neutron nuclear reactor radiation on the properties of Bragg gratings written in photosensitive Ge-doped optical fiber. *Nuclear Instruments and Methods in Physics Research, Section B: Beam Interactions with Materials and Atoms* 187, 79–86 (2002)

- [2] Wolfbeis, O.S.: Fibre-optic sensors in biomedical sciences. *Pure and Applied Chemistry* 59, 663–672 (1987)
- [3] Arregui, F.J.: *Sensors Based on Nanostructured Materials*. Springer, New York (2009)
- [4] Dakin, J., Culshaw, B.: *Optical Fiber Sensors*, vol. I, II, III and IV. Artech House Publishers, Massachusetts (1988, 1989, 1996, 1997)
- [5] Matias, I.R., Arregui, F.J., Claus, R.O.: *Optical Fiber Sensors*. American Scientific Publishers, New York (2006)
- [6] Arregui, F.J., Matías, I.R., Cooper, K.L., Claus, R.O.: Simultaneous measurement of humidity and temperature by combining a reflective intensity-based optical fiber sensor and a fiber bragg grating. *IEEE Sensors Journal* 2, 482–487 (2002)
- [7] Corres, J.M., Del Villar, I., Matias, I.R., Arregui, F.J.: Two-layer nanocoatings in long-period fiber gratings for improved sensitivity of humidity sensors. *IEEE Transactions on Nanotechnology* 7, 394–400 (2008)
- [8] Larrión, B., Hernández, M., Arregui, F.J., Goicoechea, J., Bravo, J., Matías, I.R.: Photonic Crystal Fiber Temperature Sensor Based on Quantum Dot Nanocoatings. *Journal of Sensors* (2009)
- [9] Corres, J.M., Arregui, F.J., Matías, I.R.: Sensitivity optimization of tapered optical fiber humidity sensors by means of tuning the thickness of nanostructured sensitive coatings. *Sensors and Actuators, B: Chemical* 122, 442–449 (2007)
- [10] Arregui, F.J., Liu, Y., Matias, I.R., Claus, R.O.: Optical fiber humidity sensor using a nano Fabry-Perot cavity formed by the ionic self-assembly method. *Sensors and Actuators, B: Chemical* 59, 54–59 (1999)
- [11] Homola, J.: Surface plasmon resonance biosensing. In: *CLEO/Europe - EQEC 2009 - European Conference on Lasers and Electro-Optics and the European Quantum Electronics Conference* (2009)
- [12] Homola, J.: Surface plasmon resonance biosensors: Advances and applications. In: *Proceedings of SPIE - the International Society for Optical Engineering* (2009)
- [13] Homola, J.: *Surface Plasmon Resonance Based Sensors*. Springer, New York (2006)
- [14] Gupta, B.D., Verma, R.K.: Surface plasmon resonance-based fiber optic sensors: Principle, probe designs, and some applications. *Journal of Sensors* (2009)
- [15] Gupta, B.D., Sharma, A.K.: Sensitivity evaluation of a multi-layered surface plasmon resonance-based fiber optic sensor: A theoretical study. *Sensors and Actuators, B: Chemical* 107, 40–46 (2005)
- [16] NTSC of the USA Government, "The national nanotechnology initiative. strategic plan (2004)
- [17] Fundación OPTI, "Aplicaciones industriales de las nanotecnologías en España en el horizonte 2020" (2008)
- [18] Del Villar, I., Zamarreno, C.R., Hernaez, M., Arregui, F.J., Matias, I.R.: Lossy Mode Resonance Generation With Indium-Tin-Oxide-Coated Optical Fibers for Sensing Applications. *Journal of Lightwave Technology* 28, 111–117 (2010)
- [19] Liedberg, B., Nylander, C., Lunström, I.: Surface plasmon resonance for gas detection and biosensing. *Sensors and Actuators* 4, 299–304 (1983)
- [20] van Gent, J., Lambeck, P.V., Bakker, R.J., Popma, T.H.J.A., Sudhölter, E.J.R., Reinhoudt, D.N.: Design and realization of a surface plasmon resonance-based chemo-optical sensor. *Sensors and Actuators: A. Physical* 26, 449–452 (1991)
- [21] Stenberg, E., Persson, B., Roos, H., Urbaniczky, C.: Quantitative determination of surface concentration of protein with surface plasmon resonance using radiolabeled proteins. *J. Colloid Interface Sci.* 143, 513–526 (1991)
- [22] Dougherty, G.: Compact optoelectronic instrument with a disposable sensor based on surface plasmon resonance. *Measurement Science and Technology* 4, 697–699 (1993)

- [23] Ekgasit, S., Tangcharoenbumrungsuk, A., Yu, F., Baba, A., Knoll, W.: Resonance shifts in SPR curves of nonabsorbing, weakly absorbing, and strongly absorbing dielectrics. *Sensors and Actuators, B: Chemical* 105, 532–541 (2005)
- [24] Chyou, J., Chu, C., Chien, F., Lin, C., Yeh, T., Hsu, R.C., Chen, S.: Precise determination of the dielectric constant and thickness of a nanolayer by use of surface plasmon resonance sensing and multiexperiment linear data analysis. *Appl. Opt.* 45, 6038–6044 (2006)
- [25] Chiang, H.P., Chen, C., Wu, J.J., Li, H.L., Lin, T.Y., Sanchez, E.J., Leung, P.T.: Effects of temperature on the surface plasmon resonance at a metal-semiconductor interface. *Thin Solid Films* 515, 6953–6961 (2007)
- [26] Le Person, J., Colas, F., Compere, C., Lehaitre, M., Anne, M., Boussard-Pledel, C., Bureau, B., Adam, J., Deputier, S., Guilloux-Viry, M.: Surface plasmon resonance in chalcogenide glass-based optical system. *Sensors and Actuators, B: Chemical* 130, 771–776 (2008)
- [27] Feng, W., Shenye, L., Xiaoshi, P., Zhuangqi, C., Yongkun, D.: Reflective-type configuration for monitoring the photobleaching procedure based on surface plasmon resonance. *Journal of Optics A: Pure and Applied Optics* 10 (2008)
- [28] Jorgenson, R.C., Yee, S.S.: A fiber-optic chemical sensor based on surface plasmon resonance. *Sensors and Actuators: B. Chemical* 12, 213–220 (1993)
- [29] Culshaw, B., Kersey, A.: Fiber-optic sensing: A historical perspective. *J. Lightwave Technol.* 26, 1064–1078 (2008)
- [30] Cusano, A., Lopez-Higuera, J.M., Matias, I.R., Culshaw, B.: Editorial optical fiber sensor technology and applications. *IEEE Sensors Journal* 8, 1052–1054 (2008)
- [31] Lee, B.: Review of the present status of optical fiber sensors. *Optical Fiber Technology* 9, 57–79 (2003)
- [32] Wolfbeis, O.S.: Fiber-optic chemical sensors and biosensors. *Anal. Chem.* 76, 3269–3284 (2004)
- [33] Piliarik, M., Homola, J., Manıkova, Z., Ctyroky, J.: Surface plasmon resonance sensor based on a single-mode polarization-maintaining optical fiber. *Sensors and Actuators, B: Chemical* 90, 236–242 (2003)
- [34] Gentleman, D.J., Obando, L.A., Masson, J., Holloway, J.R., Booksh, K.S.: Calibration of fiber optic based surface plasmon resonance sensors in aqueous systems. *Anal. Chim. Acta* 515, 291–302 (2004)
- [35] Mitsushio, M., Higashi, S., Higo, M.: Construction and evaluation of a gold-deposited optical fiber sensor system for measurements of refractive indices of alcohols. *Sens. Actuators A Phys.* 111, 252–259 (2004)
- [36] Kim, Y., Peng, W., Banerji, S., Booksh, K.S.: Tapered fiber optic surface plasmon resonance sensor for analyses of vapor and liquid phases. *Opt. Lett.* 30, 2218–2220 (2005)
- [37] Sharma, A.K., Jha, R., Gupta, B.D.: Fiber-Optic Sensors Based on Surface Plasmon Resonance: A Comprehensive Review. *IEEE Sensors Journal* 7, 1118–1129 (2007)
- [38] Slavık, R., Homola, J., Tyroky, J., Brynda, E.: Novel spectral fiber optic sensor based on surface plasmon resonance. *Sensors and Actuators, B: Chemical* 74, 106–111 (2001)
- [39] Rajan, Chand, S., Gupta, B.D.: Fabrication and characterization of a surface plasmon resonance based fiber-optic sensor for bittering component-Naringin. *Sensors and Actuators, B: Chemical* 115, 344–348 (2006)
- [40] Rhodes, C., Cerruti, M., Efremenko, A., Losego, M., Aspnes, D.E., Maria, J., Franzen, S.: Dependence of plasmon polaritons on the thickness of indium tin oxide thin films. *J. Appl. Phys.* 103 (2008)

- [41] Robusto, P.F., Braunstein, R.: Optical measurements of the surface plasmon of indium-tin oxide. *Physica Status Solidi (A) Applied Research* 119, 155–168 (1990)
- [42] Brewer, S.H., Franzen, S.: Optical properties of indium tin oxide and fluorine-doped tin oxide surfaces: Correlation of reflectivity, skin depth, and plasmon frequency with conductivity. *J. Alloys Compounds* 338, 73–79 (2002)
- [43] Brewer, S.H., Franzen, S.: Indium tin oxide plasma frequency dependence on sheet resistance and surface adlayers determined by reflectance FTIR spectroscopy. *J. Phys. Chem. B* 106, 12986–12992 (2002)
- [44] Yang, F., Sambles, J.R.: Determination of the optical permittivity and thickness of absorbing films using long range modes. *Journal of Modern Optics* 44, 1155–1163 (1997)
- [45] Marciniak, M., Grzegorzewski, J., Szustakowski, M.: Analysis of lossy mode cut-off conditions in planar waveguides with semiconductor guiding layer. *IEE Proc. Part J Optoelectron* 140, 247–252 (1993)
- [46] Razansky, D., Einziger, P.D., Adam, D.R.: Broadband absorption spectroscopy via excitation of lossy resonance modes in thin films. *Phys. Rev. Lett.* 95, 1–4 (2005)
- [47] Batchman, T.E., McWright, G.M.: Mode coupling between dielectric and semiconductor planar waveguides. *IEEE J. Quant. Electron.* 18, 782–788 (1982)
- [48] Carson, R.F., Batchman, T.E.: Multimode phenomena in semiconductor-clad dielectric optical waveguide structures. *Appl. Opt.* 29, 2769–2780 (1990)
- [49] Del Villar, I., Matias, I.R., Arregui, F.J., Achaerandio, M.: Nanodeposition of materials with complex refractive index in long-period fiber gratings. *J. Lightwave Technol.* 23, 4192–4199 (2005)
- [50] Xu, M.Y.C., Alam, M.Z., Zilkie, A.J., Zeaiter, K., Aitchison, J.S.: Surface plasmon polaritons mediated by ITO at near infrared wavelength. In: *Conference on Quantum Electronics and Laser Science (QELS) - Technical Digest Series* (2008)
- [51] Chopra, K.L., Das, S.R.: *Thin Film Solar Cells*. Thin Film Solar Cells. Plenum, New York (1983)
- [52] Costellamo, J.E.: *Handbook of Display Technology*. Academic, New York (1992)
- [53] Marks, R.S., Novoa, A., Konry, T., Kraus, R., Cosnier, S.: Indium tin oxide-coated optical fiber tips for affinity electropolymerization. *Materials Science and Engineering C* 21, 189–194 (2002)
- [54] Patel, N.G., Patel, P.D., Vaishnav, V.S.: Indium tin oxide (ITO) thin film gas sensor for detection of methanol at room temperature. *Sensors and Actuators, B: Chemical* 96, 180–189 (2003)
- [55] Konry, T., Novoa, A., Cosnier, S., Marks, R.S.: Development of an "electroptode" immunosensor: Indium tin oxide-coated optical fiber tips conjugated with an electropolymerized thin film with conjugated cholera toxin B subunit. *Anal. Chem.* 75, 2633–2639 (2003)
- [56] Salama, O., Herrmann, S., Tzikovsky, A., Piura, B., Meirovich, M., Trakht, I., Reed, B., Lobel, L.I., Marks, R.S.: Chemiluminescent optical fiber immunosensor for detection of autoantibodies to ovarian and breast cancer-associated antigens. *Biosensors and Bioelectronics* 22, 1508–1516 (2007)
- [57] Luff, B.J., Wilkinson, J.S., Perrone, G.: Indium tin oxide overlayers waveguides for sensor applications. *Appl. Opt.* 36, 7066–7072 (1997)
- [58] Cooper, P.R.: Refractive-index measurements of liquids used in conjunction with optical fibers. *Appl. Opt.* 22, 3070–3072 (1983)
- [59] Daimon, M., Masumura, A.: Measurement of the refractive index of distilled water from the near-infrared region to the ultraviolet region. *Appl. Opt.* 46, 3811–3820 (2007)

- [60] Lee, B., Roh, S., Park, J.: Current status of micro- and nano-structured optical fiber sensors. *Optical Fiber Technology* 15, 209–221 (2009)
- [61] Zamarreño, C.R., Hernández, M., Del Villar, I., Matías, I.R., Arregui, F.J.: Optical fiber pH sensor based on lossy-mode resonances by means of thin polymeric coatings. *Sensors and Actuators, B: Chemical*. *Sensors and Actuators, B: Chemical* 155, 290–297 (2011)
- [62] Goicoechea, J., Zamarreño, C.R., Matías, I.R., Arregui, F.J.: Optical fiber pH sensors based on layer-by-layer electrostatic self-assembled Neutral Red. *Sensors and Actuators, B: Chemical* 132, 305–311 (2008)
- [63] Itano, K., Choi, J., Rubner, M.F.: Mechanism of the pH-induced discontinuous swelling/deswelling transitions of poly(allylamine hydrochloride)-Containing polyelectrolyte multilayer films. *Macromolecules* 38, 3450–3460 (2005)
- [64] Chen, Z., Lu, C.: Humidity sensors: A review of materials and mechanisms. *Sensor Letters* 3, 274–295 (2005)
- [65] Arregui, F.J., Ciaurriz, Z., Oneca, M., Matias, I.R.: An experimental study about hydrogels for the fabrication of optical fiber humidity sensors. *Sensors and Actuators, B: Chemical* 96, 165–172 (2003)
- [66] Zamarreño, C.R., Hernaez, M., Del Villar, I., Matias, I.R., Arregui, F.J.: Tunable humidity sensor based on ITO-coated optical fiber. *Sensors and Actuators, B: Chemical* 146, 414–417 (2010)
- [67] Hernaez, M., Zamarreño, C.R., Fernandez-Valdivielso, C., Del Villar, I., Arregui, F.J., Matias, I.R.: Agarose optical fibre humidity sensor based on electromagnetic resonance in the infra-red region. *Physica Status Solidi (C) Current Topics in Solid State Physics* 7, 2767–2769 (2010)
- [68] Corres, J.M., Matías, I.R., Hernández, J.M., Bravo, J., Arregui, F.J.: Optical fiber humidity sensors using nanostructured coatings of SiO<sub>2</sub> nanoparticles. *IEEE Sensors J.* 8, 281–285 (2008)